

# Chapter 3

## The Influence of Astrocyte Activation on Hemodynamic Signals for Functional Brain Imaging

Hongbo Yu, James Schummers, and Mriganka Sur

**Abstract** Hemodynamic signals enable functional brain imaging, yet their origin and the mechanism by which they report neural activity are unresolved. Astrocytes are a major class of nonneuronal cell in the brain that receive inputs at excitatory synapses and link to the vasculature via endfeet on capillaries. Recent work utilizing in vivo high resolution cellular imaging of calcium signals in astrocytes and neurons with two-photon microscopy has revealed that astrocytes in visual cortex have sharply tuned response features that match the features of adjacent neurons. The spatially restricted, stimulus-specific, blood volume component of hemodynamic signals is exquisitely sensitive to astrocyte but not neuronal activation, demonstrating that astrocytes are responsible for a critical component of neurovascular coupling and hemodynamic signaling.

### 3.1 Brief Review of Hemodynamic Signals

Functional brain imaging relies heavily on evoked hemodynamic signals. In 1878, the Italian physiologist Mosso observed that brain pulsations over the right prefrontal cortex of a patient increased during the performance of a calculation task. Since then, multiple imaging techniques based on region-specific blood flow changes have been established and revealed various aspects of functional localization in the brain. Alongside, numerous studies have increasingly revealed details of the mechanisms that enable these forms of functional brain imaging. It has now become clear that when neuronal populations are active in any region of the brain, the region consumes more oxygen and energy immediately following activation. This oxygen consumption leads to an initial increase of local deoxyhemoglobin (dHb) (Frostig et al. 1990; Grinvald et al. 1999), followed by an increase in blood flow, carrying fresh blood with abundant supply of oxyhemoglobin (Hb). Often the late

---

M. Sur (✉)

Department of Brain and Cognitive Sciences, Picower Institute for Learning and Memory,  
Massachusetts Institute of Technology, Cambridge, MA, 02139, USA  
e-mail: msur@mit.edu

phase blood flow overcompensates the need for oxygen and causes the local dHb to be lower than baseline (Fox et al. 1988; Fox and Raichle 1986), followed by a slower return to baseline. This sequence of events, referred to as neurovascular coupling, forms the basis of modern functional brain imaging techniques, such as functional magnetic resonance imaging (fMRI) based on blood oxygen level-dependent (BOLD) signals, and intrinsic signal optical imaging.

### ***3.1.1 The BOLD Signal and Its Components***

Ogawa and Lee first took advantage of the fact that dHb is paramagnetic, and thus in the presence of dHb, the magnetic resonance signal decreases quadratically owing to the diffusion of field gradients with a concomitant variation in blood vessel contrast (Ogawa and Lee 1990; Ogawa et al. 1990a; Ogawa et al. 1990b). During activity-induced increases in local blood flow, called functional hyperemia, dHb concentration decreases seconds after brain activation and is reflected as an increase of BOLD signal in fMRI (Kwong et al. 1992; Turner et al. 1991). In detail, the primary physiological means by which neural activity causes changes in blood oxygenation are oxygen consumption (extraction) due to increased metabolic demand and increased blood flow which brings oxygen-saturated hemoglobin and also leads to increased local blood volume. The balance of these opposing processes in space and in time is the primary determinant of local hemoglobin oxygen concentration, and thus BOLD signal magnitude. Activity-driven oxygen extraction precedes activity-driven increases in blood flow, but the magnitude of the blood flow effect on dHb typically exceeds the oxygen extraction effect, so that the predominant signal measured is related to the increased blood flow. However, the extraction component (the so-called “initial dip”) can be detected under some circumstances (Buxton 2001). Increasingly refined models of these processes have been developed (Stephan et al. 2007; Friston et al. 2000; Buxton et al. 1998) and have proved generally successful in describing these phenomena quantitatively.

Since these pioneering studies, BOLD fMRI has become one of the most prominent modalities for noninvasive imaging of neural activity in human and nonhuman subjects alike. Particularly for human studies, where more invasive measurements are typically not feasible, BOLD fMRI has played a major role in our understanding of the localization of brain activity related to specific sensory, motor, and cognitive functions.

### ***3.1.2 Intrinsic Signal Imaging Relies on Similar Signals as BOLD***

Grinvald et al. (1986) found that the small evoked reflectance changes of the exposed cortex can be employed to functionally map the barrel cortex in rats and

visual cortex in cats. Brain tissue exhibits activity-dependent changes in the reflectance of specific wavelengths, which faithfully indicate neuronal activity levels. These reflectance changes depend on natural physiological processes in brain tissue and are, therefore, referred to as “intrinsic signals.” Compared to BOLD fMRI, the signals of intrinsic optical imaging are more complicated, and they include the absorption of both dHb and Hb as well as light scattering (Grinvald et al. 1999). Different components of the intrinsic signal become quantitatively more prominent when imaging at different wavelengths. This wavelength dependence can be exploited to tease apart different components of the hemodynamic signal, which are presumed to arise from distinct underlying physiological processes. For example, at certain wavelengths of green light (such as 546 nm), the absorption rates of Hb and dHb are identical, and the reflectance change at this isobestic point is closely related to the overall total hemoglobin concentration (including dHb and Hb) and thus cerebral blood volume; the activity related blood volume signal results in a decrease in reflectance. At orange to red wavelengths (such as ~600–650 nm), the absorption of dHb dominates over Hb, so that the measured signals predominantly reflect the amount of dHb. Thus, the time course of the signals measured in orange light shows a biphasic curve: the initial dip from the local deoxygenation and the subsequent upward deflection from the hyperemia seconds after stimulation (Vanzetta et al. 2004). In far-red light, where hemoglobin absorption is minimal, light scattering-induced changes in reflectance dominate the overall signal (Frostig et al. 1990), whereas in green or orange light, light scattering signals contribute less than 10% of the overall reflectance change.

### ***3.1.3 Origin and Complexity of Hemodynamic Signal Components***

The broad application of functional brain imaging techniques has facilitated neuroscience research over the last several decades; however, after many years of intensive study, the origin of the imaging signal remains largely unsolved and basic questions remain. In particular, how does local neural activity influence blood flow, and what are the mechanisms that couple neural activity to hemodynamic signals? Which aspects of neural activity (presynaptic, postsynaptic, spiking, inhibitory, excitatory, etc) are most closely related to BOLD magnitude? On what spatial scale does the neurovascular coupling occur?

It is widely accepted that vascular modulation of blood flow involves the dilatation of arterioles (Cox et al. 1993; Ngai et al. 1988), but it is not clear how the signal is delivered from neurons to neighboring blood vessels. One hypothesis is that the synaptically triggered increase of postsynaptic calcium is central to the initiation of the production of vasoactive agents (Iadecola 2004). The potential vasoactive agents include extracellular diffusible hydrogen and potassium ions (Kuschinsky and Wahl 1978; Paulson and Newman 1987), nitric oxide (Dreier

et al. 1995; Niwa et al. 1993), adenosine (Rubio and Berne 1975), and arachidonic acid metabolites (Niwa et al. 2000; Takano et al. 2006). In neocortex, some interneurons directly contact vascular processes, and the activation of these interneurons can evoke dilation or constriction of adjacent vessels in vitro (Cauli et al. 2004; Hamel 2006; Hirase et al. 2004a; Vaucher et al. 2000). On the other hand, recent studies are not in favor of a direct link between postsynaptic neurons and local blood flow: when the spiking activity of adjacent neurons is abolished in cerebellum (Mathiesen et al. 1998) or olfactory cortex (Petzold et al. 2008), the local blood flow does not decrease. Similarly, blood flow changes in visual cortex do not reflect alterations of neuronal activity but rather closely follow changes in astrocyte activation (Schummers et al. 2008; see also below). Furthermore, blood flow signals seem to be most closely related to local field potentials (Logothetis et al. 2001), and thus a large proportion of the hemodynamic signal appears to be linked to presynaptic potentials (Logothetis et al. 2001). It has been argued that this is consistent with the greater metabolic consumption involved in synaptic transmission compared with that in spiking (Iadecola 2004). It has been shown that over a narrow range, there is a linear relationship between the local field potentials and BOLD contrast signals (Hewson-Stoate et al. 2005). However, a predominant nonlinearity exists over a wider range, especially when using low stimulus intensities (Sheth et al. 2004). This complicated coupling between neural activity and hemodynamic signals makes the interpretation of functional brain imaging difficult and indicates an indirect pathway from neural activity to local blood flow control. A clear mechanistic explanation of the coupling will go a long way toward advancing our interpretation of hemodynamic imaging data in terms of the underlying neural activity.

### **3.2 Astrocytes and Their Link with Neurons and the Vasculature**

Astrocytes are known to be closely linked to blood vessels. Golgi first noticed that glial cells are connected to blood vessels either directly at the soma or at the end of long processes termed endfeet. Astrocytes send processes that extend to cover nearby synapses, as well as endfeet which contact vessel walls. Thus, anatomically, astrocytes are well positioned to link neural activity to hemodynamic activity. Furthermore, each astrocyte has its own nonoverlapping territory (Bushong et al. 2002; Bushong et al. 2003), suggesting the possibility that individual astrocytes might constitute the functional unit of neurovascular coupling. However, owing to the fact that astrocytes are electrically nonspiking (i.e., they do not generate action potentials - Volterra and Meldolesi 2005), they have long been thought to be inactive cells in the brain, whose only role is to provide metabolic support to neurons. Several recent pieces of evidence have now emerged to challenge this stereotyped role of astrocytes.

### ***3.2.1 Synaptic Inputs to Astrocytes***

Recent advances in staining methods have demonstrated that the morphology of astrocytes is closely related to neurons. Astrocytes send processes that conjoin most excitatory cortical synapses: as many as 90% of spines in somatosensory cortex are contacted by astrocytic processes (Genoud et al. 2006). Astrocyte processes can typically span ca 200  $\mu\text{m}$  and are arranged in tessellated, largely nonoverlapping domains (Bushong et al. 2003), so that a single astrocyte can make contact with more than 100,000 synapses (Bushong et al. 2002). These processes are motile on the timescale of minutes to hours. Spontaneous motility of astrocytic processes is common, and is coupled to dynamics of abutting dendritic spines (Haber et al. 2006; Hirrlinger et al. 2004). Changes in neuronal activity, *in vitro* or *in vivo*, result in remodeling of the fine structure of astrocytic processes surrounding synapses. For example, preferential stimulation of a single whisker leads to an increase in the coverage of synaptic contacts by astrocyte processes in rodent somatosensory cortex (Genoud et al. 2006). Furthermore, during development, astrocyte maturation in visual cortex correlates with the critical period for neuronal plasticity, and disruption of visual activity during this time can influence the number, morphology, and receptor expression of cortical astrocytes (Hawrylak and Greenough 1995; Muller 1990; Muller 1992; Nakadate et al. 2001). The fine structure of astrocyte morphology at synapses is likely to have important significance for synaptic transmission and plasticity. Astrocytes sense synaptic glutamate through a number of means – their processes have high concentrations of glutamate receptors and transporters, enabling them to control the kinetics of synaptic transmission by regulating the amount of glutamate available in the synaptic cleft (Anderson and Nedergaard 2003; Haydon and Carmignoto 2006).

### ***3.2.2 Activation of Calcium Signaling in Astrocytes***

In contrast to previous views of their role, it is now recognized that astrocytes are responsive to activity in nearby neurons. The major signature of astrocytic activation is mobilization of intracellular calcium. Astrocytes *in vitro* exhibit spontaneous calcium activity, which can be in the form of individual spontaneous events, oscillations, or waves. Calcium signaling can be initiated by a number of stimuli, including synaptic glutamate (Volterra and Meldolesi 2005). Brief exposure to glutamate leads to sustained calcium increases lasting several seconds following a delay or ramp time of a few seconds (Cornell-Bell et al. 1990; Porter and McCarthy 1996). In cell culture and *in vitro* slice preparations, calcium signals can propagate through the astrocytic network over distances of hundreds of microns under certain conditions (Cornell-Bell et al. 1990), though the long-range propagation may be pathological (Volterra and Meldolesi 2005). Furthermore, astrocyte calcium signaling can be differentially triggered by synaptic inputs from different sources, suggesting

that they may be involved in processing the information content of neural activity (Perea and Araque 2005).

With few exceptions, the activity of astrocytes has been characterized in vitro. With the recent combination of a specific in vivo astrocyte marker (Nimmerjahn et al. 2004) and in vivo two-photon imaging (e.g., Schummers et al. 2008), it is now possible to monitor the activity of astrocytes in vivo. The early studies using particular astrocyte labels and cellular imaging provided support for the notion that astrocytes participate in neuronal representations and processing. Astrocytes show correlated calcium waves (Hirase et al. 2004b; Nimmerjahn et al. 2004), though the propensity of astrocytes to exhibit spontaneous calcium waves in vivo under healthy conditions is open to debate (Wang et al. 2006; Takata and Hirase 2008). It has recently been demonstrated that cortical activation by sensory stimulation (whisker stimulation) can evoke calcium responses in astrocytes mediated by mGluRs (Wang et al. 2006), though an early study demonstrated astrocyte glycogen utilization following whisker stimulation (Swanson et al. 1992). Together with the in vitro evidence above, these findings suggest that astrocytes may actively sample local synaptic inputs and interact with neuronal network activity on a fine scale.

### 3.3 Role of Astrocytes in Hemodynamic Signaling

#### 3.3.1 *Astrocytes and Hemodynamic Responses*

It is well recognized that neural activation in the brain is closely coupled with vascular activity, and local hemodynamics provide the key mapping signals used for functional imaging methods such as intrinsic signal optical imaging and functional MRI (Vanzetta et al. 2005; Thompson et al. 2003; Sheth et al. 2004; Duong et al. 2001). However, until recently it has been unclear how the fast electrical activity of neurons is linked to the relatively slow vascular changes and hemodynamic signals. As described above, several kinds of evidence support the idea that astrocytes form a key link between neuronal activity and hemodynamic responses. The intrinsic optical mapping signal, for instance, has three major components. Among these, the flush-in of blood flow is the slowest signal component; it appears with a delay of a few seconds after stimulation, which is very similar to the response delay of astrocytes (Wang et al. 2006). Because astrocytes send processes to neighboring synapses and also endfeet to the local microvasculature (Simard et al. 2003), activation of astrocytes can directly modulate the dilatory state of local arterioles (Takano et al. 2006) by release of vasoactive substances such as cyclooxygenase, nitric oxide and ATP, and triggering of prostaglandin synthesis and arachidonic acid metabolites (reviewed in Haydon and Carmignoto 2006). Furthermore, in vivo work in mice reveals that the intracellular calcium concentration of astrocytes increases after whisker stimulation (Wang et al. 2006). Astrocytes may therefore regulate local blood delivery in an exquisite way, and thus directly modulate the late component of functional imaging signals.

However, this proposal is not without complexity since astrocytes are also thought to be linked together by strong gap junctional connections, and large scale calcium waves have been described in astrocytes in vitro, which in turn do not favor spatially restricted activation of astrocytes and their suggested highly localized control of blood flow. Thus, fundamental questions about the relationship between neuronal networks, astrocytes, and hemodynamic responses need to be answered: How closely matched are astrocyte responses to adjacent neuronal responses? Specifically, are the calcium responses of astrocyte narrowly or broadly tuned relative to those of adjacent neurons? Are the maps of astrocyte tuning properties (e.g., in visual cortex) sharply divided into subregions in space, as are neuronal maps? Are hemodynamic signals separable from astrocyte responses, and from neuronal responses?

### 3.3.2 *Response Specificity of Astrocytes*

The precise orderly mapping of orientation preference in visual cortex of higher mammals provides a model system to study the interactions among neurons, astrocytes, and hemodynamic responses. Neurons with similar preferred orientations cluster and form a columnar structure in primary visual cortex; preferred orientation of neuronal columns generally varies systematically and smoothly across cortical space (Fig. 3.1a), with several sparsely distributed focal regions, such as pinwheel centers, where preferred orientation changes rapidly on a scale of less than 50 microns (examples in Fig. 3.1d, also see Bonhoeffer and Grinvald 1991; Yu et al. 2005; Grinvald et al. 1999). The detailed structure of this mapping was first revealed by intrinsic signal imaging, which is based on indirect measurement of cortical electrophysiology (Grinvald et al. 1999; Frostig et al. 1990). It is remarkable that methods such as intrinsic signal optical imaging, based on putatively coarse hemodynamic signals, nonetheless provide reports of neuronal maps at high spatial resolution. More recently, in vivo two-photon calcium imaging has been applied in cortex (Stosiek et al. 2003; Helmchen and Denk 2005), by injecting a small amount of the calcium indicator dye OGB1 into the cortex and labeling all cells in a small volume (Fig. 3.1c). By inferring changes in neural firing rates from fluorescent readings of changes in calcium concentration, the visual response properties of large populations of individual neurons can be described. Thus, single cell resolution orientation maps can be obtained, and they prove to be highly precise and organized at the level of individual neurons, even at pinwheel centers (Fig. 3.1e, g–i, also see Ohki et al. 2006). Importantly, when orientation maps from neuronal calcium signals and hemodynamic signals from the same cortex are aligned carefully by local vascular pattern (Fig. 3.1b, c), they match very well spatially, even at pinwheel centers (Fig. 3.1d, e), suggesting a very precise neurovascular coupling. As a potential mediator of this coupling, understanding the response specificity of astrocytes with respect to neighboring neurons and local blood volume control is crucial.

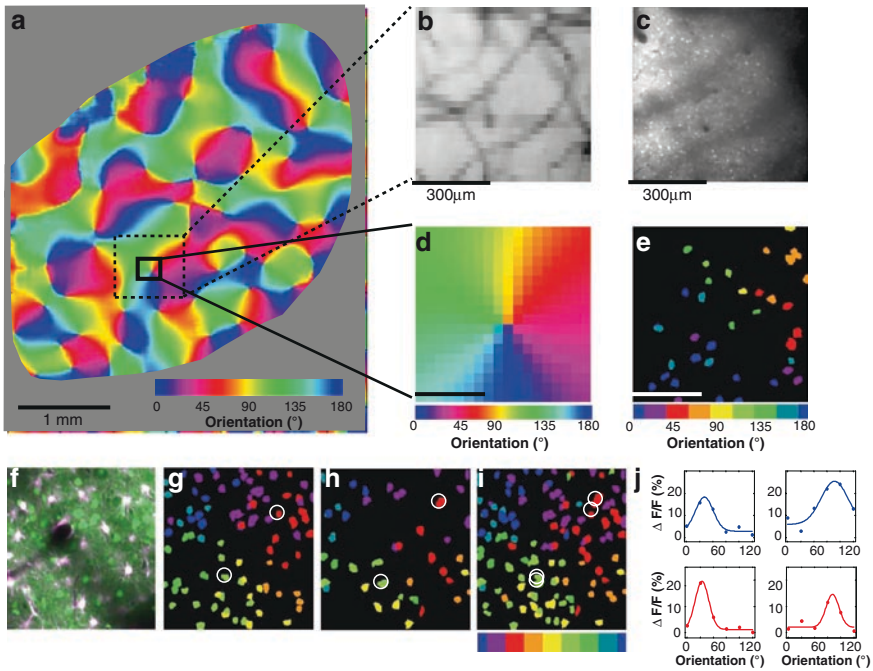


**Fig. 3.1** Matched orientation preference maps revealed by intrinsic signal imaging, and two-photon imaging of astrocytes and neurons in the ferret visual cortex. **(a)** Orientation preference map generated by intrinsic signal optical imaging. **(b)** Surface blood vessel pattern captured by the CCD camera during optical imaging, covering a region  $750\mu\text{m}$  square (indicated by the dashed box in **a**). **(c)** Fluorescence image captured with the two-photon microscope after injection of OGB1 in the region indicated in **(b)**. Note the similarity in the vascular pattern between panels **b** and **c**. **(d)** Expanded view of the orientation preference map from the small boxed area indicated in **a**. Scale bar,  $100\mu\text{m}$ . **(e)** Single cell orientation preference map of a group of neurons in the same cortical area shown in **d**. Note that the preferred orientation of the neurons closely matches that of the optical imaging signal in **d**. **(f)** Merged image of SR101 and OGB1 label in a  $250\mu\text{m}\times 250\mu\text{m}$  patch of cortex from a single plane  $120\mu\text{m}$  below the pial surface. Astrocytes appear white; neurons appear green. Scale bar,  $100\mu\text{m}$ . **(g)** Single cell-based orientation preference map for the population of neurons labeled in **(f)**. Neurons from multiple planes are included in this image. Orientation preference was determined by Gaussian fits to the data and is coded according to the scale at **(i)**. **(h)** Single cell-based orientation preference map for the population of astrocytes labeled in **(f)**. **(i)** Overlaid orientation preference map for neurons and astrocytes. **(j)** Example tuning curves from two neurons (blue traces; indicated by circles in **g**) and two astrocytes (red traces; indicated by circles in **h**)

For this purpose, parallel two-photon calcium imaging of neurons and astrocytes and optical imaging of blood volume changes was performed in primary visual cortex of ferrets (Schummers et al. 2008). Astrocytes were labeled by infiltration with the specific astrocyte marker SR101 (Nimmerjahn et al. 2004), while neurons and astrocytes were loaded with the calcium indicator OGB1. In this double labeled preparation, astrocytes and neurons are interleaved with each other in visual cortex

(Fig. 3.1f). Astrocytes do respond to visual stimuli, and the calcium elevation of the cell body is sharply tuned to the orientation of the drifting gratings, even at pinwheel centers (Fig. 3.1j). Importantly, the single cell resolution astrocyte orientation map is also highly organized with distinct pinwheel centers (Fig. 3.1h) that are as precise as that of neurons (Fig. 3.1g). The overlay of the two maps (Fig. 3.1i) shows that the alignment of the pinwheel center is matched perfectly between neurons and astrocytes. In summary, orientation maps of neurons, astrocytes, and hemodynamic signals coexist in primary visual cortex of ferret: astrocyte orientation preference maps resemble both neuronal and hemodynamic orientation maps with extremely high spatially resolution, consistent with the potential role of astrocytes in mediating the neurovascular coupling.

### 3.3.3 *Role of Astrocytes in Hemodynamic Signaling*

This similarity of the astrocyte map and the neuronal and hemodynamic maps is suggestive of a potential role for astrocytes in mediating the coupling between the latter. It is also noteworthy that the calcium response of astrocytes are delayed 2–4 s after visual stimulation (Fig. 3.2b; see Schummers et al. 2008), as also reported in barrel cortex (Wang et al. 2006). The timing of the onset astrocyte responses thus coincides with the onset of the hyperemic response, providing further correlative evidence for a role for astrocytes in this coupling. In order to dissect the influence of astrocytes more directly, hemodynamic orientation maps were measured while the activation of astrocytes was manipulated independently from neuronal activity by blocking astrocytic responses without interfering with neuronal synaptic transmission. One mechanism to trigger astrocyte responses is the activation of glutamate transporters (De Saint Jan and Westbrook 2005). Astrocyte glutamate transporters provide the major mechanism for glutamate clearance from the synaptic cleft, and their activity tightly regulates the amplitude and kinetics of synaptic transmission in vitro (Anderson and Swanson 2000). When the glutamate transporter antagonist DL-threo- $\beta$ -benzyloxyaspartate (TBOA) was applied via a visualized pipette, the responses of astrocytes were clearly and significantly reduced (Fig. 3.2a, b). The responses of neurons were unchanged or increased to a lesser extent, and some neurons which were unresponsive in the control condition become measurably responsive during TBOA application (Fig. 3.2a). Furthermore, neuronal responses were prolonged during TBOA application (Fig. 3.2b), consistent with an increase in glutamate availability at synapses, because it is not cleared by astrocyte transporters. These data demonstrate a key role for astrocytes in regulating the strength and time course of neuronal responses to incoming synaptic inputs.

Having demonstrated that TBOA is an effective means to silence astrocytes without any potential confound from reducing neuronal responses, the effects of TBOA on stimulus-specific blood volume responses was examined by intrinsic signal imaging. It is known that intrinsic signals measured at the near-isobestic green wavelength of 546 nm are closely related to the overall hemoglobin concentration

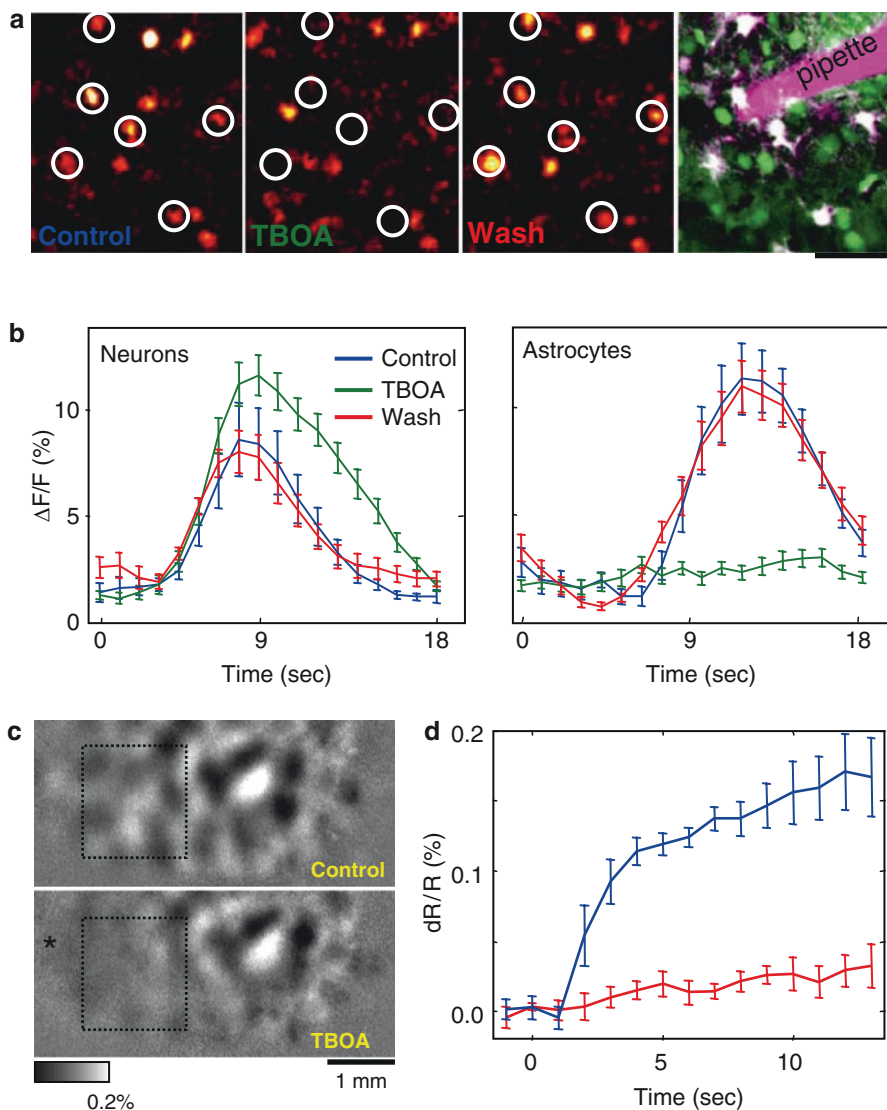


**Fig. 3.2** Astrocyte calcium responses and the intrinsic optical signal are selectively affected by the glutamate transporter antagonist TBOA. **(a)** Magnitude map for visually driven responses in a field of cells, before, during and after application of TBOA. Astrocytes are circled in *white*. Position of TBOA pipette, and dual labeling of astrocytes (*white*) and neurons (*green*) are shown in rightmost panel. **(b)** Mean ( $\pm$  SEM) responses of a population of 13 astrocytes and 25 neurons from the same experiment as in **(a)** to a continuously changing orientation stimulus, before, during, and after TBOA application. Note that the response duration of neurons is prolonged and response magnitude slightly increased during TBOA application, while the response of astrocytes is abolished. **(c)** Differential intrinsic signal maps (derived from the response to a grating at 0 degrees minus that at 90 degrees) obtained with light of 546 nm, before and during TBOA application. TBOA was applied from a cannula positioned at the \*. **(d)** Time course of the mapping signal magnitude (mean  $\pm$  SEM), calculated from the portion of the map indicated by the rectangle in **(c)**. TBOA nearly abolishes the mapping signal, as evident by the severe reduction of differential response (*contrast*) within the rectangle in **(c)** after TBOA application

and thus local blood volume (Grinvald et al. 1999; Frostig et al. 1990). Under green light, the differential map of two orthogonal stimulus orientations thus reflects the orientation-specific control of local blood volume. TBOA reduced these signals almost to baseline (Fig. 3.2c, d) – a striking effect, given that neuronal responses are actually increased following TBOA application (Fig. 3.2b). On an average, the mapping signal was reduced to a similar extent as the astrocyte calcium response. This demonstrates that blocking astrocyte calcium responses greatly weakens orientation-specific local blood volume regulation. It is of interest to know whether this weakening was due to a nonspecific, general, effect on the cortex caused by TBOA injection or a specific effect on blood volume control. To clarify this issue, the global intrinsic signals were evaluated simultaneously at two unique wavelengths. The global signals are derived from the “cocktail” signals of two orthogonal stimulus orientations, and they reflect the overall visually evoked intrinsic signals. At 546 nm, in the center of TBOA application site (Fig. 3.3a, star), the green light reflectance changed little compared to the control (Fig. 3.3a, left box; Fig. 3.3b, left), suggesting little blood volume increase evoked by the visual stimulus. Imaging under red light illumination (630 nm) emphasizes oximetric components of intrinsic signals. A typical visually driven reflectance change at this wavelength includes an initial decrease due to increased oxygen consumption, followed 2–4 s later by an upward deflection in reflectance, due to increased blood flow, which brings additional, oxygenated blood to offset the oxygen consumption (examples in Fig. 3.3c, blue curves, also see Grinvald et al. 1999; Frostig et al. 1990). Following TBOA application, close to the application site, the reflectance curve decreased monotonically (Fig. 3.3c, left, red curve), suggesting strong visually evoked consumption of oxygen in a well functioning cortex. However, the upward deflection which reflects blood flow increase disappeared (Fig. 3.3c, left), suggesting that the late increase in blood flow was dependent on astrocyte activity. Furthermore, the inflection point at 630 nm (Fig. 3.3c), which indicates the balance between oxygen consumption and additional oxygen brought by increased blood flow, occurred 2–4 s after visual stimulation, consistent with the delay of peak calcium responses in astrocytes (Figs. 3.2b, 3.4c, 3.5b). With increasing distance from the injection site, the signal at 546 nm became progressively stronger (Fig. 3.3b, middle and right panels), and the upward deflection in the signal at 630 nm gradually increased in magnitude (Fig. 3.3c). The amplitudes of the downward signal at 546 nm and upward component at 630 nm were well matched at each distance from the TBOA application site (Fig. 3.3b, c). Taken together, the effect of astrocyte glutamate transporter blockade by TBOA correlated well with the reduction of evoked blood volume increase, as revealed by the spatial and temporal resolution of activation of hemodynamic signals when investigated by both green and red light.

Instead of physical intervention by TBOA injection, we found that manipulation of the level of inhalation anesthesia of the animal can also specifically block the astrocyte calcium response. Under slightly higher isoflurane concentration, the neuronal responses were nearly unchanged whereas the astrocyte responses were sharply reduced (Fig. 3.4a, b). The time course and amplitude of the neuron response were nearly identical under both high and low concentrations (Fig. 3.4c),

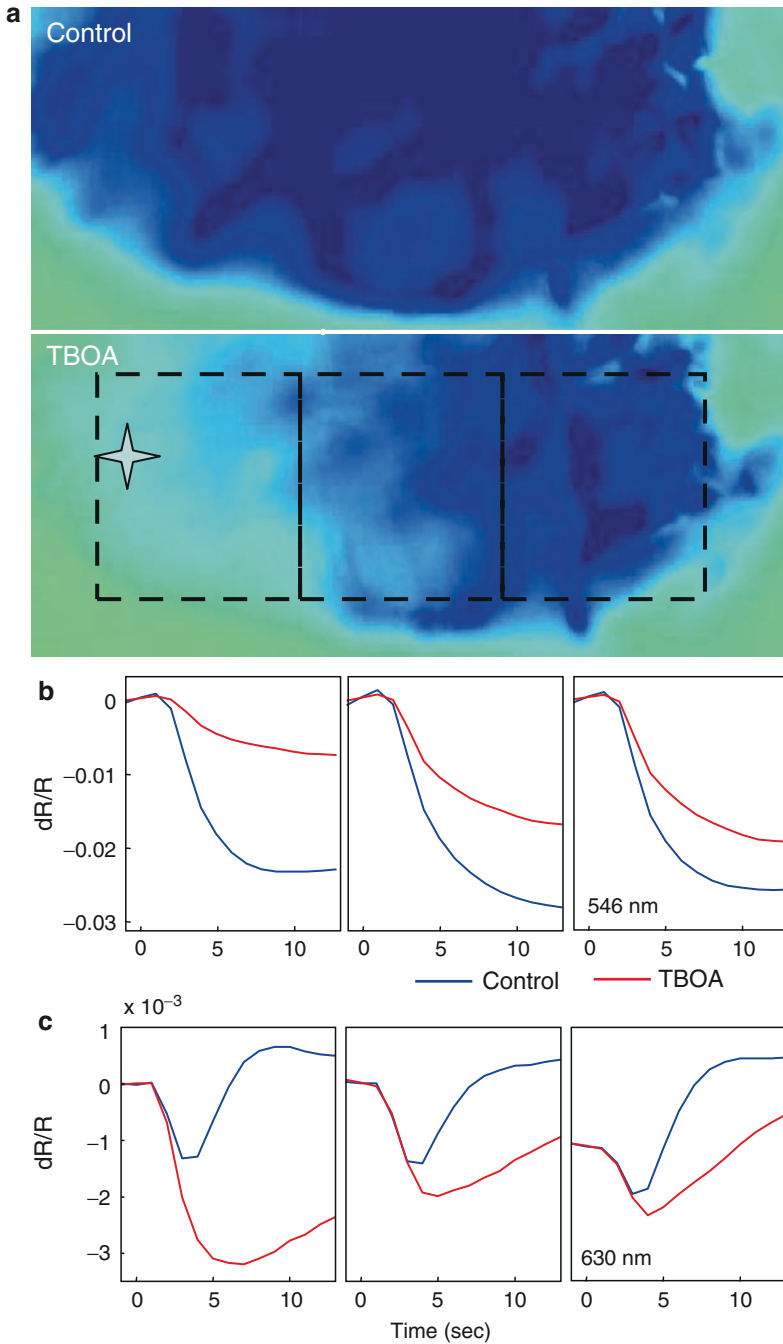


**Fig. 3.3** Spatial localization and wavelength dependence of TBOA effect on global signal in the visual cortex. **(a)** Global signal map (derived from the sum of the response to a grating at 0 degrees and that at 90 degrees) in the control condition and after TBOA application. TBOA was applied

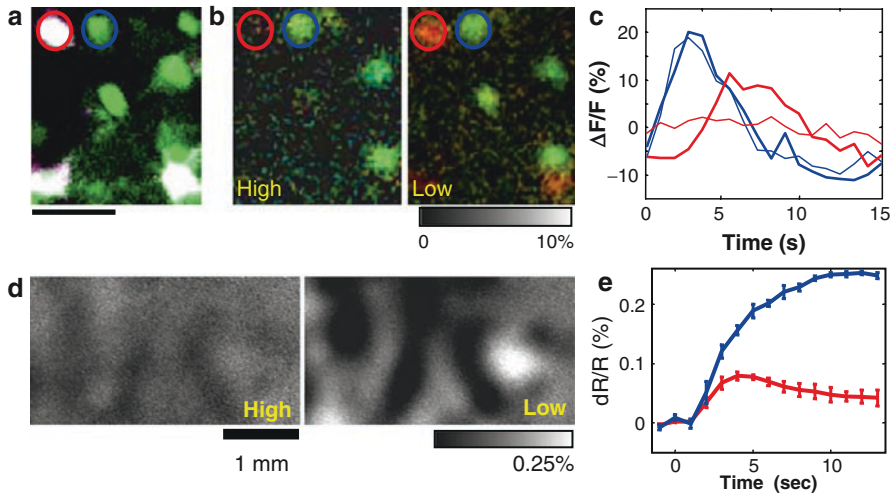


**Fig. 3.4** Astrocyte calcium responses and the intrinsic optical signal are selectively affected by increased isoflurane. (a) Merged image of SR101 and OGB1 label in a small patch of cortex. *Blue* and *red* circles mark a neuron (*labeled green*) and an astrocyte (*labeled white*), respectively. Scale bar: 50  $\mu\text{m}$ . (b) Cycle averaged visually evoked responses to a periodically rotating grating for the two cells in (a), under high (1.2%; left image) and low (0.8%; right image) concentrations of isoflurane. The images are color coded such that brightness indicates response amplitude; the amplitude bar applies to both images. (c) Orientation tuned responses of the two cells circled in (a) to a rotating grating. The neuron is plotted in *blue*, and the astrocyte in *red*. *Thick* and *thin* lines indicate low and high isoflurane, respectively. (d) Example of intrinsic signal optical imaging differential (0 minus 90 degrees) maps at 546 nm, computed from the response to 4–13 s after stimulation, during low and high isoflurane conditions. (e) Plots of the time course of reflectance change ( $dR/R$ ; mean  $\pm$  SEM) in the example shown in (d). Stimulus was turned on at time 0 s. *Blue* line depicts low isoflurane, *red* line depicts high isoflurane. Each line shows the average  $\pm$  SEM of five traces under each condition

whereas the astrocyte response was nearly abolished under high concentrations (Fig. 3.4c). Consistent with the TBOA experiments, at 546 nm, concentrations of isoflurane that preferentially reduced astrocyte responses led to a large reduction in the differential orientation maps and in the mapping signal (Fig. 3.4d, e).

The dose-dependent effects of isoflurane on the responses of neurons, astrocytes, and intrinsic signals provide further evidence for the role of astrocytes in neurovascular coupling. Small changes in isoflurane concentration, over a narrow range of concentrations around  $\sim 1\%$ , produced a modest reduction of neuronal responses but a dramatic reduction of astrocyte responses (Fig. 3.5a, b). The responses

←  
**Fig. 3.3** (continued) from a cannula positioned at the \*. (b) Time course of global signal, measured at 546 nm, from the three regions depicted in (a), demonstrating a graded effect of TBOA application. The signal after TBOA (*red curve*) is reduced compared to the control signal (*blue curve*), in particular close to the application site (*left*). (c) Time course of global signal, measured at 630 nm. The early decrease in reflectance, indicative of oxygen consumption, is unaltered. The later overshoot, caused by increased perfusion of oxygenated blood, is reduced in a graded manner

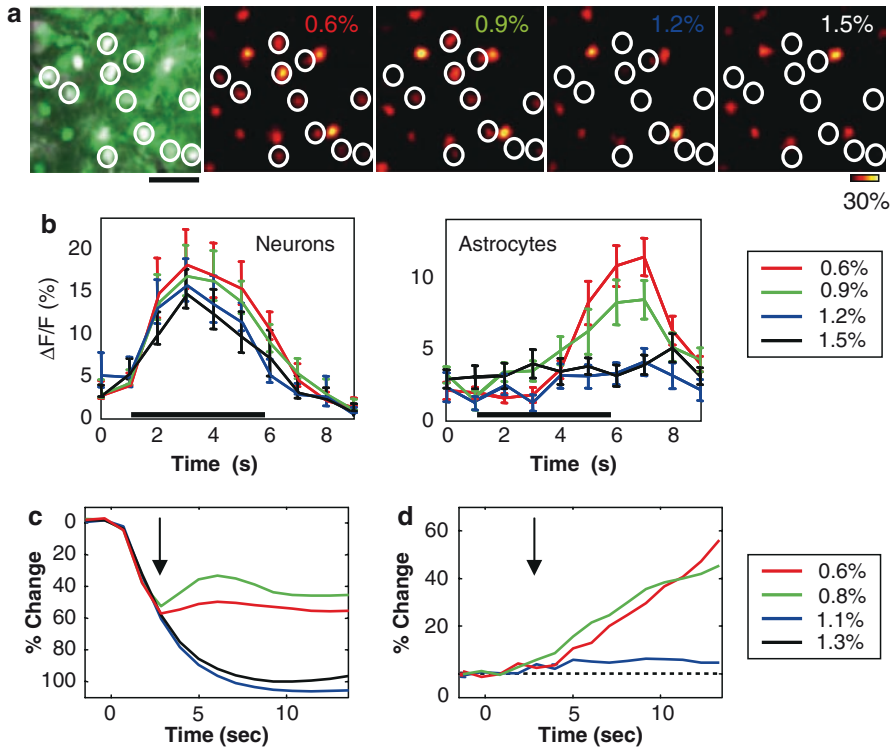


**Fig. 3.5** Astrocyte but not neuronal calcium responses are nonlinearly influenced by isoflurane in a dose-dependent manner, as is the intrinsic signal. **(a)** Dose-dependent effect of isoflurane on the responses of neurons and astrocytes. The response amplitude of a field of neurons and astrocytes at different isoflurane levels (0.6%, 0.9%, 1.2%, and 1.5%). *White circles* indicate astrocytes. Scale bar: 50  $\mu\text{m}$ . **(b)** The mean response time courses of the neurons ( $n=8$ ) and astrocytes ( $n=11$ ) from the field of view in **(a)**. Stimulus time is indicated by the *black bar*. **(c)** Plot of global intrinsic signal strength at 630 nm (shown as %, normalized by the maximal reflectance change in 1.3% isoflurane condition) as a function of time after stimulus onset under four isoflurane concentrations (red, 0.6%; green, 0.8%; blue, 1.1%; black, 1.3%). **(d)** Plot of the difference in the 630 nm mapping signal strength (% , normalized by the maximal reflectance change in 1.3% isoflurane condition) between different isoflurane concentrations (black, baseline, 1.3–1.3%; blue, 1.1–1.3%; green, 0.8–1.3%; red, 0.6–1.3%). The *arrow* in **(c)** and **(d)** shows the divergent points of intrinsic signals  $\sim 3$  s after stimulation, consistent with the astrocyte calcium response delay

of astrocytes were reduced in a dose-dependent manner, with a sharp fall-off between 0.9% and 1.2%. This suggests the possibility that a critical, high level of local neuronal activity is necessary to elicit astrocyte responses. Similar to the TBOA experiments at 630 nm (Fig. 3.3c), the divergence of the signal traces at low and high isoflurane occurred sharply at  $\sim 3$  s (arrow in Fig. 3.5c, d), which corresponds well to the delay in astrocytes responses. Importantly, two different high isoflurane concentrations (blue and black curves) had similar effects on both global and mapping intrinsic optical imaging signals, as did two different low concentrations

(red and green curves), suggesting a sharp nonlinear drop between low and high “states” around 1.0% (Fig. 3.5c, d). These effects on intrinsic signal components related to blood volume are consistent with the quasi-nonlinear effect of isoflurane on astrocyte calcium responses relative to neuronal responses.

In summary, manipulation of astrocyte responses demonstrates that in almost all aspects – including the temporal delay, spatially graded effect of TBOA injection, and dose-dependent effect of isoflurane – hemodynamic signals from local blood volume changes match astrocyte activation levels. Notably, regardless of whether the effect on neuronal responses is an increase (by TBOA) or a decrease (by isoflurane), the level of astrocyte response appears to determine the magnitude of blood volume increase, in both direct (546 nm) and indirect (630 nm) measurement. When the sharply tuned orientation selective responses of astrocytes are blocked, so that the coupling between neurons and the vasculature is broken, the mapping signal (which is highly orientation selective) is greatly decreased. These findings clearly demonstrate the key role of astrocytes as critical mediators of neurovascular coupling. The activation of neurons is necessary for obtaining strong functional imaging signals related to blood volume changes, but this influence is mediated by astrocytes and is thus secondary to astrocyte activation. The patterns of evoked blood volume signals follow those of astrocytes than neurons – a conclusion that helps elucidate some previous findings in the literature.

## 3.4 Conclusions and Outstanding Issues

### 3.4.1 *Astrocytes and Neurovascular Coupling*

Previously, it was believed that the blood volume component of intrinsic signals was regulated with low spatial precision, exceeding the size of individual neuronal functional modules in cortex, and therefore was less suitable for high resolution imaging than oximetric signals (Grinvald et al. 1999). However, high quality functional maps derived from blood volume changes have been obtained under green light in several intrinsic signal imaging experiments in auditory cortex (Versnel et al. 2002; Dinse et al. 1997), as well as in visual cortex as shown here. We conclude that a key variable is to keep astrocyte responses intact. Similarly, although there is still debate on whether an initial dip (from an early increase of dHb) exists in the fMRI BOLD signal (Buxton 2001), it is clear that the majority of the BOLD signal originates from the late stage hyperemia; thus the activation of astrocytes is essential for BOLD signal imaging. Intrinsic signal optical imaging differs slightly from BOLD signal imaging in that there are multiple sources for the intrinsic signal, and some components may not be regulated by astrocytes. For example, light scattering signals under red light (810 nm) decrease but still remain largely intact shortly after inactivation of astrocytes (our unpublished data), though the chronic effect remains unknown. It is notable, however, that the signal with green light is more than 40 times greater in absolute magnitude than that at 810 nm.

The coupling between neuronal activity and hemodynamic response magnitude is found to be linear only over a narrow range (Hewson-Stoate et al. 2005); strong nonlinearities are also seen, which are better described by a threshold or power law relationship (Sheth et al. 2004). These complexities can be explained at least partially by the nonlinear response properties of astrocytes, which have a higher threshold of activation than neurons (Schummers et al. 2008). Thus, the spatial precision and sharp tuning of astrocyte responses allow the spatially selective control of local blood volume of individual functional modules, and the thresholded responses of astrocytes help explain the nonlinear nature of neurovascular coupling. Therefore, the activity of astrocytes is critical for obtaining robust mapping signals for hemodynamic imaging, and manipulations (in addition to isoflurane and TBOA) that influence the functional state of astrocytes are likely to influence such imaging. It follows that maintaining astrocytes in a healthy condition is a critical step in functional brain imaging such as intrinsic signal imaging and fMRI of BOLD signals.

### ***3.4.2 Neural Activity, Astrocyte Activity, and Hemodynamic Response Parameters***

While understanding the role of astrocytes in neurovascular coupling is informative from a mechanistic point of view, a more detailed, quantitative, description of the role of astrocytes in neurovascular coupling will be essential to improve the interpretation of hemodynamic imaging data. The data described above are highly suggestive of a nonlinear, thresholded transformation between neuronal activity and astrocyte calcium responses. This transformation should be studied in more detail and parametrically. How much synaptic activity is required to elicit a measurable astrocyte response? Over what ranges is this relationship linear, and how can the nonlinearities be modeled? It is also noteworthy that calcium signaling in astrocyte processes may play a role in neurovascular coupling, which was not addressed with somatic measurements alone.

The transformation at the other end of the coupling – from astrocyte to vascular also warrants further quantitative study. How much calcium signal in an astrocyte is necessary to elicit a measurable hemodynamic response? How linear is this relationship? Ultimately, we may hope that with adequate characterization of astrocyte activation in relationship to both neural and vascular responses, we will obtain a quantitative understanding of the transformation from neural activity to the commonly measured parameters in hemodynamic imaging modalities.

### ***3.4.3 Effects of Anesthesia on Astrocyte Responses***

It is clear that anesthesia can alter both neuronal and astrocyte behavior. Our data described above, and those of others (Takano et al. 2006), suggest that astrocytes

may be particularly susceptible to anesthetics. If we are to be able to apply our understanding derived from anesthetized preparations to awake, especially human, subjects, we will need to assure ourselves that the same principles apply. More work will need to be done in awake animal preparations in order to bridge this gap. Recent advances on multiple fronts (Greenberg et al. 2008; Goense and Logothetis 2008; Dombek et al. 2007) promise to promote this effort in the near future.

## References

- Anderson CM, Nedergaard M (2003) Astrocyte-mediated control of cerebral microcirculation. *Trends Neurosci* 26:340–344 author reply 344–345
- Anderson CM, Swanson RA (2000) Astrocyte glutamate transport: review of properties, regulation, and physiological functions. *Glia* 32:1–14
- Bonhoeffer T, Grinvald A (1991) Iso-orientation domains in cat visual cortex are arranged in pinwheel-like patterns. *Nature* 353:429–431
- Bushong EA, Martone ME, Jones YZ, Ellisman MH (2002) Protoplasmic astrocytes in CA1 stratum radiatum occupy separate anatomical domains. *J Neurosci* 22:183–192
- Bushong EA, Martone ME, Ellisman MH (2003) Examination of the relationship between astrocyte morphology and laminar boundaries in the molecular layer of adult dentate gyrus. *J Comp Neurol* 462:241–251
- Buxton RB (2001) The elusive initial dip. *Neuroimage* 13:953–958
- Buxton RB, Wong EC, Frank LR (1998) Dynamics of blood flow and oxygenation changes during brain activation: the balloon model. *Magn Reson Med* 39:855–864
- Cauli B, Tong XK, Rancillac A, Serluca N, Lambolez B, Rossier J, Hamel E (2004) Cortical GABA interneurons in neurovascular coupling: relays for subcortical vasoactive pathways. *J Neurosci* 24:8940–8949
- Cornell-Bell AH, Finkbeiner SM, Cooper MS, Smith SJ (1990) Glutamate induces calcium waves in cultured astrocytes: long-range glial signaling. *Science* 247:470–473
- Cox SB, Woolsey TA, Rovainen CM (1993) Localized dynamic changes in cortical blood flow with whisker stimulation corresponds to matched vascular and neuronal architecture of rat barrels. *J Cereb Blood Flow Metab* 13:899–913
- De Saint Jan D, Westbrook GL (2005) Detecting activity in olfactory bulb glomeruli with astrocyte recording. *J Neurosci* 25:2917–2924
- Dinse HR, Godde B, Hilger T, Reuter G, Cords SM, Lenarz T, Von Seelen W (1997) Optical imaging of cat auditory cortex cochleotopic selectivity evoked by acute electrical stimulation of a multi-channel cochlear implant. *Eur J Neurosci* 9:113–119
- Dombek DA, Khabbaz AN, Collman F, Adelman TL, Tank DW (2007) Imaging large-scale neural activity with cellular resolution in awake, mobile mice. *Neuron* 56:43–57
- Dreier JP, Korner K, Gorner A, Lindauer U, Weih M, Villringer A, Dirnagl U (1995) Nitric oxide modulates the CBF response to increased extracellular potassium. *J Cereb Blood Flow Metab* 15:914–919
- Duong TQ, Kim DS, Ugrubil K, Kim SG (2001) Localized cerebral blood flow response at sub-millimeter columnar resolution. *Proc Natl Acad Sci USA* 98:10904–10909
- Fox PT, Raichle ME (1986) Focal physiological uncoupling of cerebral blood flow and oxidative metabolism during somatosensory stimulation in human subjects. *Proc Natl Acad Sci USA* 83:1140–1144
- Fox PT, Mintun MA, Reiman EM, Raichle ME (1988) Enhanced detection of focal brain responses using intersubject averaging and change-distribution analysis of subtracted PET images. *J Cereb Blood Flow Metab* 8:642–653
- Friston KJ, Mechelli A, Turner R, Price CJ (2000) Nonlinear responses in fMRI: the Balloon model, Volterra kernels, and other hemodynamics. *Neuroimage* 12:466–477

- Frostig RD, Lieke EE, Ts'o DY, Grinvald A (1990) Cortical functional architecture and local coupling between neuronal activity and the microcirculation revealed by *in vivo* high-resolution optical imaging of intrinsic signals. *Proc Natl Acad Sci USA* 87:6082–6086
- Genoud C, Quairiaux C, Steiner P, Hirling H, Welker E, Knott GW (2006) Plasticity of astrocytic coverage and glutamate transporter expression in adult mouse cortex. *PLoS Biol* 4:e343
- Goense JB, Logothetis NK (2008) Neurophysiology of the BOLD fMRI signal in awake monkeys. *Curr Biol* 18:631–640
- Greenberg DS, Houweling AR, Kerr JN (2008) Population imaging of ongoing neuronal activity in the visual cortex of awake rats. *Nat Neurosci* 11:749–751
- Grinvald A, Lieke E, Frostig RD, Gilbert CD, Wiesel TN (1986) Functional architecture of cortex revealed by optical imaging of intrinsic signals. *Nature* 324:361–364
- Grinvald A, Shoham D, Shmuel A, Glaser D, Vanzetta I, Shtoyerman E, Slovlin H, Arieli A (1999) *In vivo* optical imaging of cortical architecture and dynamics. In: *Modern techniques in neuroscience research* (Windhorst U, Johansson H, eds), pp 893–969. New York: Springer.
- Haber M, Zhou L, Murai KK (2006) Cooperative astrocyte and dendritic spine dynamics at hippocampal excitatory synapses. *J Neurosci* 26:8881–8891
- Hamel E (2006) Perivascular nerves and the regulation of cerebrovascular tone. *J Appl Physiol* 100:1059–1064
- Hawrylak N, Greenough WT (1995) Monocular deprivation alters the morphology of glial fibrillary acidic protein-immunoreactive astrocytes in the rat visual cortex. *Brain Res* 683:187–199
- Haydon PG, Carmignoto G (2006) Astrocyte control of synaptic transmission and neurovascular coupling. *Physiol Rev* 86:1009–1031
- Helmchen F, Denk W (2005) Deep tissue two-photon microscopy. *Nat Methods* 2:932–940
- Hewson-Stoate N, Jones M, Martindale J, Berwick J, Mayhew J (2005) Further nonlinearities in neurovascular coupling in rodent barrel cortex. *Neuroimage* 24:565–574
- Hirase H, Creso J, Buzsaki G (2004a) Capillary level imaging of local cerebral blood flow in bicuculline-induced epileptic foci. *Neuroscience* 128:209–216
- Hirase H, Qian L, Bartho P, Buzsaki G (2004b) Calcium dynamics of cortical astrocytic networks *in vivo*. *PLoS Biol* 2:E96
- Hirrlinger J, Hulsman S, Kirchhoff F (2004) Astroglial processes show spontaneous motility at active synaptic terminals *in situ*. *Eur J Neurosci* 20:2235–2239
- Iadecola C (2004) Neurovascular regulation in the normal brain and in Alzheimer's disease. *Nat Rev Neurosci* 5:347–360
- Kuschinsky W, Wahl M (1978) Local chemical and neurogenic regulation of cerebral vascular resistance. *Physiol Rev* 58:656–689
- Kwong KK, Belliveau JW, Chesler DA, Goldberg IE, Weisskoff RM, Poncelet BP, Kennedy DN, Hoppel BE, Cohen MS, Turner R (1992) Dynamic magnetic resonance imaging of human brain activity during primary sensory stimulation. *Proc Natl Acad Sci USA* 89:5675–5679
- Logothetis NK, Pauls J, Augath M, Trinath T, Oeltermann A (2001) Neurophysiological investigation of the basis of the fMRI signal. *Nature* 412:150–157
- Mathiesen C, Caesar K, Akgoren N, Lauritzen M (1998) Modification of activity-dependent increases of cerebral blood flow by excitatory synaptic activity and spikes in rat cerebellar cortex. *J Physiol* 512(Pt 2):555–566
- Muller CM (1990) Dark-rearing retards the maturation of astrocytes in restricted layers of cat visual cortex. *Glia* 3:487–494
- Muller CM (1992) Astrocytes in cat visual cortex studied by GFAP and S-100 immunocytochemistry during postnatal development. *J Comp Neurol* 317:309–323
- Nakadate K, Imamura K, Watanabe Y (2001) Effects of monocular deprivation on the expression pattern of alpha-1 and beta-1 adrenergic receptors in the kitten visual cortex. *Neurosci Res* 40:155–162
- Ngai AC, Ko KR, Morii S, Winn HR (1988) Effect of sciatic nerve stimulation on pial arterioles in rats. *Am J Physiol* 254:H133–H139
- Nimmerjahn A, Kirchhoff F, Kerr JN, Helmchen F (2004) Sulforhodamine 101 as a specific marker of astroglia in the neocortex *in vivo*. *Nat Methods* 1:31–37

- Niwa K, Lindauer U, Villringer A, Dirnagl U (1993) Blockade of nitric oxide synthesis in rats strongly attenuates the CBF response to extracellular acidosis. *J Cereb Blood Flow Metab* 13:535–539
- Niwa K, Araki E, Morham SG, Ross ME, Iadecola C (2000) Cyclooxygenase-2 contributes to functional hyperemia in whisker-barrel cortex. *J Neurosci* 20:763–770
- Ogawa S, Lee TM (1990) Magnetic resonance imaging of blood vessels at high fields: in vivo and in vitro measurements and image simulation. *Magn Reson Med* 16:9–18
- Ogawa S, Lee TM, Kay AR, Tank DW (1990a) Brain magnetic resonance imaging with contrast dependent on blood oxygenation. *Proc Natl Acad Sci USA* 87:9868–9872
- Ogawa S, Lee TM, Nayak AS, Glynn P (1990b) Oxygenation-sensitive contrast in magnetic resonance image of rodent brain at high magnetic fields. *Magn Reson Med* 14:68–78
- Ohki K, Chung S, Kara P, Hubener M, Bonhoeffer T, Reid RC (2006) Highly ordered arrangement of single neurons in orientation pinwheels. *Nature* 442:925–928
- Paulson OB, Newman EA (1987) Does the release of potassium from astrocyte endfeet regulate cerebral blood flow? *Science* 237:896–898
- Perea G, Araque A (2005) Properties of synaptically evoked astrocyte calcium signal reveal synaptic information processing by astrocytes. *J Neurosci* 25:2192–2203
- Petzold GC, Albeanu DF, Sato TF, Murthy VN (2008) Coupling of neural activity to blood flow in olfactory glomeruli is mediated by astrocytic pathways. *Neuron* 58:897–910
- Porter JT, Mccarthy KD (1996) Hippocampal astrocytes in situ respond to glutamate released from synaptic terminals. *J Neurosci* 16:5073–5081
- Rubio R, Berne RM (1975) Regulation of coronary blood flow. *Prog Cardiovasc Dis* 18:105–122
- Schummers JR, Yu H, Sur M (2008) Tuned responses of astrocytes and their influence on hemodynamic signals in the visual cortex. *Science* 320:1638–1643
- Sheth SA, Nemoto M, Guiou M, Walker M, Pouratian N, Toga AW (2004) Linear and nonlinear relationships between neuronal activity, oxygen metabolism, and hemodynamic responses. *Neuron* 42:347–355
- Simard M, Arcuino G, Takano T, Liu QS, Nedergaard M (2003) Signaling at the gliovascular interface. *J Neurosci* 23:9254–9262
- Stephan KE, Weiskopf N, Drysdale PM, Robinson PA, Friston KJ (2007) Comparing hemodynamic models with DCM. *Neuroimage* 38:387–401
- Stosiek C, Garaschuk O, Holthoff K, Konnerth A (2003) In vivo two-photon calcium imaging of neuronal networks. *Proc Natl Acad Sci USA* 100:7319–7324
- Swanson RA, Morton MM, Sagar SM, Sharp FR (1992) Sensory stimulation induces local cerebral glycogenolysis: Demonstration by autoradiography. *Neuroscience* 51:451–461
- Takano T, Tian GF, Peng W, Lou N, Libionka W, Han X, Nedergaard M (2006) Astrocyte-mediated control of cerebral blood flow. *Nat Neurosci* 9:260–267
- Takata N, Hirase H (2008) Cortical layer 1 and layer 2/3 astrocytes exhibit distinct calcium dynamics in vivo. *PLoS ONE* 3:e2525
- Thompson JK, Peterson MR, Freeman RD (2003) Single-neuron activity and tissue oxygenation in the cerebral cortex. *Science* 299:1070–1072
- Turner R, Le Bihan D, Moonen CT, Despres D, Frank J (1991) Echo-planar time course MRI of cat brain oxygenation changes. *Magn Reson Med* 22:159–166
- Vanzetta I, Sloviter H, Omer DB, Grinvald A (2004) Columnar resolution of blood volume and oximetry functional maps in the behaving monkey; implications for fMRI. *Neuron* 42:843–854
- Vanzetta I, Hildesheim R, Grinvald A (2005) Compartment-resolved imaging of activity-dependent dynamics of cortical blood volume and oximetry. *J Neurosci* 25:2233–2244
- Vaucher E, Tong XK, Cholet N, Lantin S, Hamel E (2000) GABA neurons provide a rich input to microvessels but not nitric oxide neurons in the rat cerebral cortex: a means for direct regulation of local cerebral blood flow. *J Comp Neurol* 421:161–171
- Versnel H, Mossop JE, Mrcic-Flogel TD, Ahmed B, Moore DR (2002) Optical imaging of intrinsic signals in ferret auditory cortex: responses to narrowband sound stimuli. *J Neurophysiol* 88:1545–1558

- Volterra A, Meldolesi J (2005) Astrocytes, from brain glue to communication elements: the revolution continues. *Nat Rev Neurosci* 6:626–640
- Wang X, Lou N, Xu Q, Tian GF, Peng WG, Han X, Kang J, Takano T, Nedergaard M (2006) Astrocytic  $\text{Ca}^{2+}$  signaling evoked by sensory stimulation in vivo. *Nat Neurosci* 9:816–823
- Yu H, Farley BJ, Jin DZ, Sur M (2005) The coordinated mapping of visual space and response features in visual cortex. *Neuron* 47:267–280